



UNIVERSITY OF LEEDS

This is a repository copy of *A three-dimensional numerical model of borehole heat exchanger heat transfer and fluid flow*.

White Rose Research Online URL for this paper:
<http://eprints.whiterose.ac.uk/89701/>

Version: Accepted Version

Article:

Rees, SJ orcid.org/0000-0003-4869-1632 and He, M (2013) A three-dimensional numerical model of borehole heat exchanger heat transfer and fluid flow. *Geothermics*, 46. pp. 1-13. ISSN 1879-3576

<https://doi.org/10.1016/j.geothermics.2012.10.004>

© 2012 Elsevier Ltd. Licensed under the Creative Commons Attribution-NonCommercial-NoDerivatives 4.0 International <http://creativecommons.org/licenses/by-nc-nd/4.0/>

Reuse

Unless indicated otherwise, fulltext items are protected by copyright with all rights reserved. The copyright exception in section 29 of the Copyright, Designs and Patents Act 1988 allows the making of a single copy solely for the purpose of non-commercial research or private study within the limits of fair dealing. The publisher or other rights-holder may allow further reproduction and re-use of this version - refer to the White Rose Research Online record for this item. Where records identify the publisher as the copyright holder, users can verify any specific terms of use on the publisher's website.

Takedown

If you consider content in White Rose Research Online to be in breach of UK law, please notify us by emailing eprints@whiterose.ac.uk including the URL of the record and the reason for the withdrawal request.



eprints@whiterose.ac.uk
<https://eprints.whiterose.ac.uk/>

A three-dimensional numerical model of borehole heat exchanger heat transfer and fluid flow

Simon J. Rees*^a, Miaomiao He^a

a) Institute of Energy and Sustainable Development, De Montfort University, Leicester, UK.

Corresponding Author:

Simon Rees sjrees@dmu.ac.uk

Institute of Energy and Sustainable Development, De Montfort University, The Gateway,
Leicester, LE1 9BH, UK. +44 (0)116 257 7976

Keywords: borehole heat exchanger; numerical model, conduction, fluid flow

A three-dimensional numerical model of borehole heat exchanger heat transfer and fluid flow

Abstract

Common approaches to the simulation of Borehole Heat Exchangers assume heat transfer within the circulating fluid and grout to be in a quasi-steady state and ignore axial conduction heat transfer. This paper presents a numerical model that is three-dimensional, includes explicit representations of the circulating fluid and other borehole components, and so allows calculation of dynamic behaviours over short and long timescales. The model is formulated using a finite volume approach using multi-block meshes to represent the ground, pipes, fluid and grout in a geometrically correct manner. Validation and verification exercises are presented that use both short timescale data to identify transport delay effects, and long timescale data to examine the modelling of seasonal heat transfer and show the model is capable of predicting outlet temperatures and heat transfer rates accurately. At long timescales borehole heat transfer seems well characterized by the mean fluid and borehole wall temperature if the fluid circulating velocity is reasonably high but at lower flow rates this is not the case. Study of the short timescale dynamics has shown that nonlinearities in the temperature and heat flux profiles are noticeable over the whole velocity range of practical interest. The importance of representing the thermal mass of the grout and the dynamic variations in temperature gradient as well as the fluid transport within the borehole has been highlighted. Implications for simplified modelling approaches are also discussed.

Nomenclature

C_p	specific heat (kJ/kg.K)
D	diameter (m)
E	East
F	cell face flux (W/m ²)
h	convection heat transfer coefficient (W/m ² .K)
L	length (m)
\mathbf{n}	surface normal vector (-)
P	Point (in mesh)
Q	heat transfer rate per unit length (W/m)
r	radius (m)
R	thermal resistence (m.K/W)
S	surface area (m ²)
t	time (s)
T	temperature (°C)
\mathbf{v}	surface velocity vector (m/s)

\dot{v} volume flow rate (m³/s)

V volume (m³)

Greek Symbols

α thermal diffusivity (m²/s)

ξ local coordinates (m)

ρ density (kg/m³)

Γ thermal conductivity (W/m.K)

τ non-dimensional time (-)

subscripts

i cell index

e east

w west

n north

s south

t top

b bottom

superscripts

C convection

D diffusion

n convection correlation exponent

Numbers

Nu Nusselt number

Re Reynolds number

Pr Prantl number

Acronyms

BHE Borehole Heat Exchanger

BiCGSTAB Bi-conjugate gradient stabilized solver

CARM Capacitance Resistance Model

CFD Computational Fluid Dynamics

DST Duct Storage model

EWS Erdwärmesonden

GEMS3D General Elyptical Mult-block Solver 3D

HVAC Heating Ventilation and Air-conditioning

RMSE Root Mean Square Error

RTD Residence time distribution

TRCM Thermal Resistance Capacitance Model

TRNSYS Transient System simulation tool

TRT Thermal Response Testing

1. Introduction

Single pairs of pipes formed in a 'U' loop and grouted into vertical boreholes are probably the commonest form of ground heat exchanger found in Ground Source Heat Pump systems, and are known as Borehole Heat Exchangers (BHEs). The components of

such a heat exchanger are illustrated in Fig. 1. BHEs of this type are not only used in building heating and cooling systems but in large thermal storage schemes also. The primary physical phenomena of interest in the study of heat exchanger performance are the dynamic conduction in the pipe, grout and surrounding ground as well as convection at the pipe wall. In reality, the heat transfer in the surrounding ground may be enhanced by groundwater flow through porous and possibly fractured rock. If interaction with the heat-pump system and its controls is to be considered then it becomes necessary to consider the physics of variable flow and diffusion of heat in the circulating fluid.

It is not common, nor always necessary, to include representation of all these physical processes in BHE models. This may be partly a practical consideration of what physical parameter data are available (or measurable) as well as the level of detail required to meet the modelling objective. Models of BHEs have three principle applications namely (i) design of BHEs – determining the required borehole depth, number of boreholes etc.; (ii) analysis of in-situ ground thermal response test (TRT) data; and (iii) integrated building and system simulation i.e. with the model coupled to HVAC and building thermal models to study overall system performance.

A number of analytical, numerical and hybrid models exist and the features of a number are reviewed here. These models differ mostly according to whether they consider three spatial dimensions, multiple boreholes, groundwater convection and buoyancy effects, heterogeneous thermal properties, grout and pipe thermal capacity and explicit representation of transport of heat by the circulating fluid.

The question of dimensionality and to what level of detail the grout, pipe and fluid components are represented bears a relationship to both the timescales and length scales that have to be considered. At short timescales, being able to resolve the dynamic changes in temperature gradient within the borehole is essential to determining fluid temperatures. At long timescales (a number of years), it is necessary to consider conduction in the surrounding ground in the axial (third) dimension. This is because – particularly if an array of boreholes is considered – conduction below the borehole, and towards the ground surface further from the borehole, become more significant after a number of years of operation. This was demonstrated in the early work of Eskilson (1987) who applied an axial-radial 2D numerical model to capture axial conduction effects and an analytical superposition method to consider interaction between

neighbouring boreholes in the horizontal direction. The importance of axial heat transfer is has been commented upon by Marcotte *et al.* (2010) and has also been recognised in more recent application of analytical finite line source models (Zeng *et al.* 2002, Molina-Giraldo *et al.* 2011) although in these models interaction between neighbouring boreholes is neglected.

If only medium and long timescales are considered – as they are in the ‘g-function’ response factor models of Eskilson (1987) and Hellström (1991) – then the borehole can be considered a single resistive element. This can be argued to be sufficient for applications of the model for design purposes where it is more important to consider long-term responses, particularly where annual heating and cooling demands are not well balanced. Eskilson stated that g-function data derived using his approach should only be applied at timescales such that $t > 5r_b^2/\alpha$. This limit may amount to a number of days. If shorter timescales are to be considered – as they need to be where system simulation is the objective – it may be sufficient to consider heat transfer in two-dimensions, and possibly only the radial direction. At shorter time scales, behaviour is strongly dependent on the dynamic behaviour of the borehole pipe, grout and fluid components. Hybrid approaches whereby different models are applied depending on time scale can be devised to treat the whole range of timescales. For example, a one-dimensional numerical model was added to the response factor approach in the DST model (Hellström 1991) to allow simulation in the TRNSYS simulation environment (SEL, 1997).

Yavuzturk and Spitler (1999) used a two dimensional numerical model of a borehole (Yavuzturk *et al.* 1999) to calculate short timescale responses and subsequently extend g-function response data to allow short simulation time steps (as short as a few minutes) to be simulated. Several studies have been carried out using this ‘short time step g-function’ model (Gentry *et al.*, 2006; Sankaranarayanan, 2005) and the model has been implemented in the EnergyPlus simulation environment (Fisher *et al.*, 2006). Yavuzturk’s numerical model (1999) represented the pipes as ‘pie sector’ shapes and did not include an explicit representation of the circulating fluid. Young (2004) sought to address this by applying a ‘buried cable’ analogy to include the effect of the fluid’s thermal capacity. Xu and Spitler (2006) sought to simplify the derivation of short

timescale response data further by developing an equivalent one-dimensional numerical model that includes the thermal mass of the fluid.

As variation in fluid temperature according to depth cannot be considered explicitly in two-dimensional models such as those discussed above, some assumption has to be made about the fluid temperatures associated with the two pipes and their relationship to the inlet and outlet temperatures. For example, both pipes could be assumed to be at a temperature equivalent to the average of the inlet and outlet temperatures. An alternative is to assume one pipe temperature is the same as that of the inlet and the other is at the outlet temperature. These assumptions can be avoided in a three-dimensional numerical model where temperature variation with depth can be considered explicitly.

In some ground source heat pump systems, depending on the dynamic load profile, the minimum and maximum operating fluid temperatures are a dominant consideration in the design and control of the system. These extreme temperatures can occur on very short timescales, for example, where capacity control is by switching the heat pump cyclically on and off. Extreme temperatures may be exhibited on timescales of a few hours in intermittently occupied buildings such as churches. The importance of such short timescale effects, and their impact on the operation of the control system, were demonstrated in a simulation study of a hybrid domestic system by Kummert and Bernier (2008) and measurements of a larger non-residential system by Naiker and Rees (2011). It is apparent that at such short timescales, or generally at higher frequencies of inlet temperature variation, the response at the BHE outlet is far from instantaneous and peaks in outlet temperature are both damped and delayed. This is also indicated in the experimental data presented later in this paper. Accurately predicting peak or minimum temperatures is therefore an important modelling issue in some important applications.

Damping of the inlet temperature fluctuations can be accounted for partly by the observation that, particularly in non-residential systems with larger diameter distribution pipes, the total thermal capacity of the fluid in the U-tubes and interconnecting pipes is relatively large – probably of the same order as that of the grout in all the boreholes. The physical process that has a further effect on the short timescale response is the dynamic transport of the circulating fluid and thermal diffusion along the

pipes. This could be expected to be important at short timescales if one considers that the nominal transit time of the fluid travelling through the U-tube could be of the order of a few minutes with typical BHE depths and pipe velocities. Variations in inlet temperature are diffused because fluid does not circulate in a 'plug' with uniform velocity but fluid at the centre of the pipe travels at higher velocity than the fluid near the pipe wall. Hence, fluid at the outlet will generally have been mixed with fluid in the pipe that entered the heat exchanger at an earlier time and probably at a different temperature. Both the thermal mass of the fluid and the diffusive transport process mean that swings in inlet temperature tend to be damped. Such effects can also be expected to be more noticeable in systems with variable flow. In such systems, the transport delay could be several minutes when the flow is reduced to minimum levels during part load conditions.

A number of BHE models include an explicit representation of fluid circulation but stop short of complete three-dimensional discretization. Some models make other simplifications in order to limit the total number of equations to be solved. For example, Wetter and Huber's EWS model (1997) is discretized vertically so that a series of fluid nodes are included but the heat transfer in the grout is represented by a single lumped capacitance and conduction is assumed radial only. Oppelt *et al.* (2010) have sought to address this limitation of the EWS model by dividing the grout into sectors so that each vertical layer of a double U-tube was represented by five lumped thermal capacitances. De Carli *et al.* (2010) developed a so-called Capacity Resistance Model (CaRM) and discretized the borehole – including the circulating fluid – into several slices along its depth with each slice also discretized in the radial direction. They also proposed modifying the outer boundary conditions to allow whole borehole arrays to be modelled.

Bauer *et al.* (2011) used a simplified representation of the borehole components in the form of a network of resistances and capacitances in the TRCM model and discretized the borehole in the vertical direction in a similar way to the EWS and CaRM models. Fluid responses and vertical temperature gradients calculated over short timescales using this model compared favourably with those from a fully discretized finite element model. These network or simplified finite difference models could be thought of as quasi-three-dimensional and have the advantage that fluid transport is

explicitly represented but are limited in not being able to calculate axial heat transfer outside the borehole and hence not able to represent all long timescale effects.

Where three-dimensional numerical models have been applied, the interest has mostly been in studying long time and spatial scales, for example, interaction in larger borehole arrays, heterogeneous ground properties or the effects of groundwater flow. In view of the computational demands of such methods, a number of approaches have been proposed to reduce the discretization of the borehole components. Al-Khoury *et al.* (2005, 2006) developed a special 1D heat pipe finite element that considered the pipe flows and conduction in the grout material using a single element. The borehole fields of interest were discretized using a vertical line of such elements coupled to surrounding 3D elements. A very similar approach was developed by Diersch *et al.* (2011) to integrate a BHE in a commercial finite element software package and similarly, Signorelli *et al.* (2007). Mottaghy and Dijkshoorn (2012) have taken a similar approach except that the borehole is represented by a finite difference model coupled to the 3D finite element solver. Cui *et al.* (2008) used a commercial finite element solver but discretized the grout and pipes with a relatively fine mesh of 3D elements. Although their treatment of the fluid is not fully described the predictions of heat transfer rates and pipe wall temperature compared favorably with short timescale experimental measurements.

One approach to modelling BHE with the aim of capturing all the physical effects noted earlier, is to use a three dimensional numerical model that discretizes the borehole components and includes a discrete dynamic model of the circulating fluid. This is the approach taken in the work reported here. Three-dimensional models have the advantage that dynamic fluid transport along the pipe loop can be represented explicitly and temperature variations according to depth can be modelled. In addition, different layers of rock and soil can be explicitly represented and climate dependent boundary conditions at the surface can be applied. Furthermore, heat transfer below the borehole array can be explicitly considered and initial vertical ground temperature gradients can be imposed.

Three-dimensional models offer most generality and potentially most accurate representation of heat transfer but have the disadvantage that considerable computing resources are required for transient simulation over extended timescales. The model

presented here has consequently been used to make generic studies of BHE behaviour and to calculate response function data over the full range of short and long timescales. Although the model has been used in annual simulation this would not be practical for most users. The model has been presented in briefer form, and for particular applications, in He *et al.* (2010) and more fully in He (2012). The intention has also been to use the model as a reference so that the limitations of simpler two-dimensional models can be better understood and an improved model developed. This is reported elsewhere.

In this paper, we describe the underlying numerical method and the approach taken to discretize the BHE and surrounding ground. The model has been validated in a number of ways. The model's ability to accurately calculate the conduction around the pipes within the borehole, and generally to deal with non-orthogonal meshes, is verified with reference to analytical conduction heat transfer solutions. The limitations of the approach taken to model the transport of fluid along the pipe are also studied with reference to an analytical solution. More than one year of experimental data has been used to validate the ability of the model to calculate seasonal heat balances and high frequency data to study the significance of the fluid circulation on short timescale dynamic response. Later in this paper, we present a numerical study of borehole vertical temperature and heat flux profiles under a range of fluid flow conditions.

2. Model development

A dynamic three-dimensional numerical model of BHEs has been developed, built upon a finite volume solver known as GEMS3D (General Elliptical Multi-block Solver 3D) which is an in-house code implemented in Fortran 90. The GEMS3D solver has been used to model ground heat exchanger problems in a number of earlier projects (Deng *et al.*, 2005; Rees *et al.*, 2002) and further details are given in He (2012). Model verification and validation of this solver has been reported elsewhere by Young (2004) and Fan and Rees (2009). The model has similarities with the finite volume model presented by Li and Zheng (2009) except that the mesh extends to include the pipe and fluid rather than stopping at the outside of the pipe.

2.1 The numerical method

The Finite Volume Method has been used to discretize the integral form of the convection-diffusion temperature equation. The approach to dealing with non-orthogonal cell geometries has been to discretize the equation in physical space using an approach similar to that described by Ferziger and Peric (2002). The primary variables are defined at the hexahedral cell centroids on a block-structured mesh. The integral form of the convection-diffusion equation solved here (leaving aside source terms) is:

$$\frac{\partial}{\partial t} \int_V \rho C_p T dV + \int_S \rho C_p T \mathbf{v} \cdot \mathbf{n} dS = \int_S \Gamma \nabla T \cdot \mathbf{n} dS \quad (1)$$

We explain the discretization of the convective and diffusive flux terms separately as follows. The advection flux term in discrete form is approximated by the sum of the convection (advection) fluxes through each cell face such that,

$$\int_S \rho C_p T \mathbf{v} \cdot \mathbf{n} dS \approx \sum_i F_i^C \quad (2)$$

where, $i = n, s, w, e, t, b$ for a hexahedral cell. Assuming the flux can be represented by the values of temperature and velocity at the cell face centroid, we can use the face area and normal vector to make the second order approximation,

$$F_i^C = (\rho C_p T \mathbf{v} \cdot \mathbf{n})_i S_i \quad (3)$$

In this particular implementation of the heat exchanger model the convection (advection) flux term is only used for simulating the fluid flows in the pipes and only the velocity in the downward and upward directions in the associated cells is non-zero. Again, assuming that the value of the temperature T over a particular face is well represented by the value at the face centroid, the diffusion heat flux can be approximated as

$$F_i^D = \int_{S_i} \Gamma \nabla T \cdot \mathbf{n} dS \approx (\Gamma \nabla T \cdot \mathbf{n})_i S_i \quad (4)$$

This requires a discrete method for finding the gradient of the temperature (∇T) at each cell face using the cell centroid values. A typical non-orthogonal cell, with local coordinates at the east cell face, is illustrated in Fig. 2. The coordinate n is defined in the

direction normal to the face at its centroids, and the coordinate ξ is defined on the line between neighboring centroids which passes through the face at point e' .

In order to calculate the gradient of the variable at the cell face, the values of the variable at the cell centroids are used as they are the primary variables. The gradient is calculated using the values T_P and T_E at neighboring centroids and the distance between these points, $L_{P,E}$ (in Fig. 2 at the east face $F_e^D \approx \Gamma_e S_e (\partial T / \partial \xi)_{e'}$) but this is only second-order accurate if the grid is orthogonal. In order to preserve second-order accuracy the calculation of the gradient along the normal to the face at the centroid needs to be made using the values at points P' and E' . However, the values of the temperature at these points are not calculated explicitly and have to be interpolated from the cell centroid values. Consequently a 'deferred correction' approach is used to calculating the flux as follows:

$$F_e^D = \Gamma_e S_e \left(\frac{\partial T}{\partial \xi} \right)_{e'} + \Gamma_e S_e \left[\left(\frac{\partial T}{\partial n} \right)_e - \left(\frac{\partial T}{\partial \xi} \right)_{e'} \right]^{old} \quad (5)$$

During the iterative solution process, the terms in the square brackets are calculated from the previous estimates of the variables. When the solution is converged the first and the third terms cancel each other to leave the term that only uses the gradient along the face normal. Central differencing is used to estimate the gradients:

$$\left(\frac{\partial T}{\partial \xi} \right)_{e'} = \frac{(T_E - T_P)}{L_{P,E}} \quad \text{and} \quad \left(\frac{\partial T}{\partial n} \right)_e = \frac{(T_{E'} - T_{P'})}{L_{P',E'}} \quad (6)$$

Values at the locations P' and E' are interpolated from the cell centroid values using the gradient of the variable which, in turn, can be calculated from the face centroid values by applying Gauss theorem (Ferziger and Peric, 2002). Temporal discretization can be first or second order backwards implicit using a method that allows for variable time steps (Singh and Bhadauria, 2009).

The sets of algebraic equations arising from the discretization on the multi-block mesh are solved using an iterative method based on the Strongly Implicit Procedure (Stone, 1968) adapted to allow communication of data across block boundaries during the iterative procedure and has been found to be very robust. A BiCGSTAB solver is also available for strongly convective problems. Using a block-structured approach also

allows a degree of parallel processing by the solving the equations of each block with separate threads.

2.2 Mesh generation

The borehole heat exchanger geometry has been discretized using a three-dimensional multi-block boundary fitted structured mesh and this has been defined using an in-house utility (Rees, 2009) that uses a two-dimensional definition of the borehole components and extrudes this to form a 3D mesh such as that shown in Fig. 3. Individual blocks define the pipes and two blocks are used to define the grout material within the borehole. Multiple blocks may be used to define the surrounding ground depending on the far field boundary shape and also – by repeating similar borehole block arrangements – adjacent boreholes. In this paper only a single borehole is studied and a semi-circular far field boundary is sufficient. (Applications with multi-borehole meshes are described in He, 2012). Coarse and fine borehole meshes are illustrated in Fig. 4.

The fluid circulating in the U-tube is represented as a single layer of cells in the mesh adjacent to the inner pipe surfaces. This is all that is required to implement a fully coupled one-dimensional model of the fluid transport. The thermal capacity of these cells is adjusted so that the fluid mass of the whole pipe is taken into consideration. The inlet boundary condition is defined by the velocity and temperature at the cell faces at the top of the pipe and the fluid velocity is imposed in each cell along the length of the pipes according to the time varying mass flow rate. This approach amounts to a one dimensional representation of the fluid flow. The limitations of this approximation are discussed later.

Heat transfer by conduction within the circulating fluid is not significant compared to the convection processes. The convective heat transfer between the fluid and the pipe wall is modeled according to the Dittus-Boelter equation,

$$Nu = 0.023Re^{4/5}Pr^n \quad (7)$$

where $n = 0.4$ for heating and 0.3 for cooling. The convection coefficient can then be found according to,

$$h = \frac{0.023Re^{4/5}Pr^n \cdot \Gamma}{D} \quad (8)$$

The conductance of the fluid cells is accordingly modified to achieve the correct relationship between fluid and pipe wall temperatures at each time step according to the mass flow rate.

3. Model validation

The ability of the model to calculate transient heat transfer rates over both short and long timescales has been validated by a combination of analytical and experimental analysis. The accuracy of the fluid transport model has been evaluated by reference to analytical solutions for adiabatic pipe flow. Calculation of conduction within the borehole has been verified by reference to analytical solutions of the steady-state borehole thermal resistance. Finally, experimental data has been used to validate the model's predictions of heat transfer rates on both short and long timescales.

3.1 Fluid transport

The representation of the circulating fluid in this model, whereby the fluid entering each control volume is transported at the temperature upstream, can be considered similar to a Compartments-In-Series model of pipe flow (Wen and Fan, 1975). Fluid transport models of this type have been widely used in process engineering and their characteristics are well known. Hanby *et al.* (2002) analysed this type of model both with and without convective heat transfer and evaluated a finite-difference discretization by making comparisons with an adiabatic analytical solution based on that of Bosworth (1949). The BHE model of fluid transport has been assessed in a similar manner.

The transport properties of a pipe (be it heat or a chemical species that is transported) can be thought of in terms of Residence Time Distribution (RTD). The RTD is considered as the fraction of fluid, which undergoes a step change at the inlet, appears in the outgoing fluid at time t , and it is represented by the function $F(t)$, illustrated in a F -Diagram. The analysis is simplified by using dimensionless time given by,

$$\tau = \frac{\dot{v}t}{V} \quad (9)$$

The actual shape of the F -Diagram depends primarily on the velocity profile. In general, the faster-moving fluid near the pipe centreline will arrive at the end of the pipe more

quickly than the bulk of the fluid. At the same time, fluid near the pipe wall travels at a velocity lower than the mean. The circulating fluid undergoes a diffusion process so that step changes in inlet condition appear smoothed at the outlet. The model's ability to reproduce this phenomenon can be evaluated by comparing the transient temperature response at the outlet to a step change at the inlet with the analytically calculated RTD.

The F-Diagram predicted by the model is shown in Fig. 6. These results have been calculated using 60 cells along the length of the pipe and using two different temporal discretization schemes. These are first order and second order backwards implicit schemes (Singh and Bhadauria, 2009). The solutions are compared with the analytical solution (Hanby *et al.*, 2002; Bosworth, 1949). The first order scheme slightly over-predicts the diffusion of the flow and the second order scheme less so.

Hanby *et al.* (2002) found that the predicted RTD had some dependence on the number of cells (compartments) used to represent the pipe. This has also been found with this BHE model. This effect can be evaluated by calculation of the differences between the predicted temperatures and the analytical F-function. The Root Mean Square Error (RMSE) for two different temporal discretization schemes over the range $0.8 < \tau < 1.5$ for different number of cells is shown in Fig. 6.

Using the first order backwards implicit scheme the error drops quickly from 20 to 60 cells, and approaches 0.08 for more than 60 cells. Using the second order approximation the error reaches a minimum with 47 cells. These results are consistent with the findings of Hanby *et al.* (2002). In practical calculations, 60 – 80 cells have been used to discretize the borehole in the vertical direction and the first order scheme has been adopted (being more robust) so that errors of this type in the range 0.07 – 0.08 could be expected.

It should be noted that the model always tends to over-predict the degree of diffusion. Although the error is greater than one would like it should be noted that this cannot be addressed to any great degree by higher order differencing schemes. The model accuracy is limited primarily by the fact that the two-dimensional flow in the pipe is assumed to be one-dimensional. This might be addressed by CFD calculation of the pipe fluid flow (i.e. solution of the Navier-Stokes equations) but this would add unreasonable computational burden. Some overestimation of the diffusion process is acceptable as further diffusion occurs in real borehole arrays by virtue of the horizontal

header pipes. We suggest that other models that use a one-dimensional discretization of the fluid (e.g. 1D finite elements or finite difference approximations) are likely to show similar levels of accuracy and possibly mesh dependence.

3.2 Borehole conduction

There is no exact analytical solution for three-dimensional heat transfer in a borehole geometry that can be applied to try to validate a numerical model. However, if only conduction in two dimensions is considered, calculation of steady-state borehole thermal resistance can be used as a metric to validate the model. Young (2004) carried out an extensive study to compare the steady state borehole resistances calculated using a number of models, including Paul's method (1996), the Gu and O'Neal's approximate diameter method (1998) and the multipole method (Bennet *et al.*, 1987). These results were compared with numerical results using a 2D version of the GEMS3D solver. The multipole method can be regarded as a reference method and accurate to within machine precision. A similar comparison of numerical model results with values of borehole thermal resistance calculated using the multipole method is presented below. This comparison is a useful validation exercise in that it tests the ability of the numerical method to deal with the curved pipe and grout boundary geometry.

Assuming the heat transfer of BHEs is in steady-state, the total amount of heat transfer rate per unit length between the fluid and the ground can be expressed as:

$$Q = \frac{T_f - T_b}{R_b} \quad (10)$$

The borehole resistance defined here includes the convective resistance between the fluid and the inner side of the pipes, the conductive resistance of the pipes, and the conductive resistance of the grout. Values of borehole thermal resistance can be found from the numerical model by making a steady-state calculation of the heat flux across the borehole wall and borehole temperature for a given fluid and far field temperature difference. Two single BHEs with different borehole diameters and two different grout types have been studied. The borehole dimensions and thermal properties are shown in Table 1.

In principle, a numerical method should produce results approaching the analytical values of conductance as the mesh is refined. Accordingly, to verify the model,

borehole thermal resistance has been calculated with a range of mesh densities. The calculated borehole thermal resistances are shown in Table 2 for meshes with numbers of cells in a two-dimensional plane of between 656 and 40,448 cells (see Fig. 4). The model can be seen to be capable of matching with the analytical values found using the multipole method (Bennet *et al.*, 1987) to within 0.1%. Variation of mesh density from 656 to 40,448 cells shows very small changes in terms of borehole thermal resistance. In practical calculations, using coarser meshes to reduce computation times would be reasonable.

3.2 Experimental validation

Data obtained from an experimental facility at Oklahoma State University have been used to validate the numerical calculations of overall heat transfer rates and outlet temperature response over short and long timescales. The experimental facility was designed and constructed to study hybrid ground source heat pump systems (Hern, 2004) and the measured data from the ground loop have been used here. The same data set has been used in a ground heat exchanger inter-model comparative study by Spitler *et al.* (2009). The borehole dimensions and properties are shown in Table 3. The ground thermal conductivity value was taken as the mean of three values determined by Thermal Response Tests.

In these experiments the inlet and outlet fluid temperatures of the BHEs were measured at 1 minute intervals over 18 months. The three boreholes are spaced far enough apart so that no thermal interaction could be expected during this initial operating period and so the data can be interpreted as representing the behavior of a single borehole. In the following validation exercises the measured inlet temperature and mass flow rate have been used as model boundary conditions and outlet temperatures and heat transfer rates have been compared with values predicted by the model.

3.2.1 Validation over short timescales

In order to study the predictions of short timescale response and examine the significance of fluid transport effects, minutely data for the first month of the experiment have been compared with predicted values. During the experiments the heat pump was

switched on and off intermittently and the circulating pump ran continuously. Data showing two cycles of operation in the 15th day of operation (March 15, 2005) are shown in Figs 7 and 8. When the heat pump switches on (time 15:11) the inlet temperature falls quickly by approximately 3K. The experimental results show that there is no response observable at the outlet until 5 minutes later. Later in the operating cycle the outlet temperature falls at a similar rate to that of the inlet. At the end of the operating cycle (15:50) the inlet temperature shows a sharp increase and a similar delay in the outlet temperature response can be observed. The delay in the response is of the same magnitude as the nominal transit time of the U-tube which, at the flow rate in question, is 4.4 minutes. Very similar trends can be seen in the subsequent cycle of operation shown in Fig. 8.

The outlet temperature predicted by the numerical model can be seen to demonstrate very similar delays in response at both the beginning and the end of heat pump operation. The response at the end of heat pump operation is slightly more damped than that shown in the experimental data. During the operating period the outlet temperature prediction follows the experimental data closely. The Root Mean Square Error (RMSE) for the predicted outlet temperature data shown in Figs. 7 and 8 is 0.324K and 0.320K respectively.

The significance of modeling the fluid circulation has been highlighted by including data from a related two-dimensional model in Figs. 7 and 8. This model is reported in detail in He (2012) and uses the same numerical solver and similar mesh density but only one cell in depth. The outlet temperature in this and other 2D models necessarily responds instantly (although damped by the thermal mass of the grout) to changes in inlet temperature. The outlet temperature predicted by this 2D model can, accordingly, be seen to respond to the changes in inlet temperature without any observable delay. Other models that do not explicitly represent the fluid flow could be expected to respond in a similar manner to this 2D model. The significance of these effects could be expected to be greater at lower velocities and in variable flow rate systems (He *et al.*, 2010).

3.2.2 Validation over Long Timescales

In order to study the predictions of heat rejection and temperature response over long timescales, hourly data for the whole 18 months of the experiment have been used as boundary conditions to the model. The predictions of mean monthly heat exchanger outlet temperature are shown along with the related experimental data in Fig. 9. The RMSE in the monthly mean outlet temperature prediction over this period is 0.57K. The differences are greatest in the month of December (1.4K) and the following August (1.5K). In other months the error is much less than the RMSE value.

Predicted Monthly net heat exchanges are compared with values derived from the experimental data in Fig. 10. In most months the predicted values are less than the experimental values. The exceptions to this are in the months of April of the first year and March of the second year. The greatest discrepancies are during the winter period.

Similar comparisons, for a number of models, were presented by Spitler *et al.* (2009). Most of the models tested showed the most significant differences also occurred in the mid winter period. One possible explanation of this trend offered by the authors was that this period corresponded with the occasions where heat pump operation was more intermittent i.e. operating cycles were shorter and there were no loads for longer periods. They also note that cyclic operation was not well represented in the hourly data when the cycles were less than one hour in duration. We suggest that one further complicating factor may be the influence of the horizontal header pipes connecting the three boreholes. Although these pipes are short relative to the total pipe length they are more likely to be influenced by atmospheric conditions. All the models, including the one presented here, ignore any influence of heat transfer at the ground surface and all horizontal pipes.

4. Vertical temperature and heat flux profiles

One of the features and advantages of a three dimensional model such as this, is that temperature and heat flux variations with depth are explicitly calculated. We have, further to the validation exercises reported above, made a numerical study of the behavior of a BHE with respect to temperature and heat flux variation within the borehole and their variation with depth. Of particular interest have been the relationships between fluid temperatures and the inlet and outlet temperatures, variation in flux and temperature at the borehole wall and also the significance of the

heat fluxes between the two legs of the U-tube. Variations with respect to fluid circulation rates have been of further interest.

These aspects of BHE behavior are partly of interest as different assumptions are made about these relationships in simpler models. Again, some distinction can be made between short and long timescale behavior and the following discussion is separated accordingly. In these studies a single BHE with a borehole diameter of 150mm and a depth of 100m has been simulated. The grout thermal conductivity was 0.75 W/m.K and other parameters are as shown in Table 1. The surrounding ground to a diameter of 4 metres has been included in the simulation domain.

4.1 Long timescale profiles

To investigate thermal behavior of a BHE at long timescales in a generic manner we have made a series of calculations with steady-state boundary conditions. These conditions are also representative of conditions at long timescales where step response is being considered. In these calculations the inlet and far-field boundary temperatures and the fluid flow rate have been fixed. A 10K difference between inlet and far field temperature has been applied and calculations made for fluid mean velocities in the range 0.2-1.0 m/s. A fluid velocity of 0.6 m/s is thought to be representative of a well designed BHE with reasonable pressure drops. 1.0 m/s is thought to be towards the upper limit of what may be found in practice. This velocity is typical of building systems but may result in unreasonable pressure drops. Flow velocities at the lower end of this range are of interest as they may occur in systems with variable speed pumping. This lower limit should still result in fully turbulent flow. Even lower flow rates that result in laminar flow may occur in variable flow systems. The flow rates and Reynolds Numbers and convection coefficients that apply over this velocity range are shown in Table 4.

The fluid temperature variations along the two legs of the U-tube are shown in Fig.11 and the corresponding temperature at the borehole wall in Fig.12. This borehole wall temperature has been found from the average around the circumference of the borehole at a given depth. Over much of the flow rate range the fluid temperature profiles (Fig.11) are approximately linear and the fluid temperature at the bottom of the borehole is representative of the mean. At lower flow rates the profile is noticeably non-linear, particularly at the bottom of the velocity range (0.2 m/s). At this flow rate there is

a greater temperature change along the pipe with downward flow (the pipe forming the inlet) than the other.

At the highest flow rate the temperature at the borehole wall (Fig.12.) varies very little. At lower flow rates (0.2-0.4 m/s) non-linear variation of borehole temperature with depth is noticeable. The corresponding heat fluxes across the borehole wall are shown in Fig.13. In this type of calculation the heat fluxes are driven by the temperature differences between the fluid and the borehole wall. Although there is an approximately linear variation of fluid temperature at higher flow rates, the mean fluid temperature at a particular depth is nearly the same. Hence, the flux along the borehole at higher flow rates is nearly constant. At low flow rates this is not the case and a noticeably non-linear profile can be seen.

Due to the temperature difference between the upward and downward fluid in adjacent pipes, some heat is transferred directly from one pipe to the other, rather than the borehole wall. (This inter-tube heat flux is sometimes referred to as the 'short-circuit' heat flux.) The inter-tube heat flux could be expected to be proportional to the temperature difference between the upward and downward flowing fluids at a given depth in steady conditions. This is reflected in the heat fluxes shown in Fig.14. This flux is naturally highest at the top of the borehole where this fluid temperature difference is greatest and lowest at the bottom. Fig. 11 showed the greatest temperature differences near the top of the borehole at the lowest flow rate. The inter-tube flux is, accordingly, shown in Fig.14 to be highest at the lowest flow rate. At the highest flow rate this flux represents approximately 2% of the total borehole heat transfer and at the lowest flow rate this is increased to 10%.

Some observations regarding modeling practice can be made based on these results. Models that do not include an explicit representation of the components of the borehole but define the relationship between the fluid temperature and borehole wall temperature by a single thermal resistance (e.g. g-function models such as that in EnergyPlus (Fisher *et al.* 2006), often assume the fluid temperature to be the mean of the inlet and outlet values and that conditions are constant along the borehole. The linear and symmetrical temperature profile and the constant borehole wall conditions shown in the results for higher flow rates suggest that this is a reasonable assumption.

At lower flow rates this is not the case and another modeling approach should probably be considered.

In a two-dimensional numerical model, for example that of Yavuzturk *et al.* (1999), some assumption has to be made about the temperature boundary condition applied at each pipe. The same mean temperature is found whether the pipe temperatures are assumed to be the inlet and outlet temperatures, or whether they are both assumed to be at the mean condition. However, one assumption will result in an over-prediction of the inter-tube flux and the other a zero inter-tube flux. Neither of these assumptions seems appropriate in light of the results reported above. One interpretation of the linear profiles shown in some results would be that the temperature boundary conditions applied at the pipes should correspond to that half way along the borehole. This would be equivalent to $\frac{1}{4}$ and $\frac{3}{4}$ of the difference between the inlet and outlet temperatures relative to the inlet. Again, this may not be appropriate at low flow rates.

4.2 Short timescale profiles

It has already been shown that, at short timescales, the dynamic response of the grout and the transport of fluid around the pipes can have a significant effect on the response of the heat exchanger. Short timescale variations in temperature and heat flux profile have been studied by making transient calculations and applying a step boundary condition to the inlet temperature. In these calculations the inlet is increased 10K above the initial state and results are presented for a range of nominal circulating fluid transit times up to 3.0. A step response boundary condition is of practical interest because many systems are controlled by turning the heat pump on and off intermittently.

The temperature profiles vary with time but also with fluid circulating velocity or flow rate. Results for fluid velocities of 1.0m/s, 0.6m/s and 0.2m/s are shown in Figs. 15 – 17 respectively. In all cases the fluid temperature profile at the earliest times ($\tau=0.3$) changes much more, and in a noticeably non-linear manner, in the downward flowing tube. As time progresses (towards $\tau=3$) the fluid temperature profile can be seen to develop into a more linear and equally divided form. In the case with low fluid velocity (Fig. 17) the non-linear nature of the temperature profile persists.

The dynamic changes in fluid temperature profile at these short timescales are a function of the simultaneous transient conduction through the pipe and grout and also the transport of fluid along the pipe. The coupling between the fluid and the pipe/grout is also changed slightly by the reduction in heat transfer coefficient at lower flow rates. At normalized times of 0.3 and 0.6 there has been very little increase in the outlet temperature. This is consistent with the residence time distribution shown in Fig.5 and therefore suggests that the transport delay accounts for much of these effects at the very shortest timescales. As time progresses dynamic conduction between the fluid and the borehole becomes the more dominant effect.

The borehole heat flux profile for the case with a fluid velocity of 0.6 m/s is shown in Fig.18. It is noticeable that the profiles are less linear than they were in the steady-state (Fig 13). The heat fluxes change very little during the initial stages of the step change. At the latest time shown ($\tau=3$) the fluxes have reached approximately 20% of the steady-state value. It can also be seen that the variation in flux along the borehole wall (at a particular time) is not as significant as the variation in fluid temperatures.

These trends can be explained by considering the role of the thermal mass of the grout between the pipes and the borehole wall. The thermal mass of the grout damps out and delays the effect of the short timescale changes in inlet fluid temperature. The fact that the temperatures in one leg of the U-tube can be very different than those in the other at short timescales is consequently not reflected in the temperature variations at the borehole wall in these calculations.

It is interesting to consider the BHE overall heat transfer rate. This could be considered by reference to the summation of the heat fluxes along the borehole wall but also by reference to the inlet-outlet fluid temperature difference at a particular time. If the fluxes at the borehole wall are considered (Fig.18) the flux rises slowly towards the steady value. In contrast, if the fluid temperatures are considered, as the outlet temperature – due to the transport delay – does not increase for some minutes the heat transfer rate defined by the fluid heat balance will appear very large and, in fact, larger than the steady-state value. At later times the heat transfer rate at the borehole wall approaches the value indicated by the fluid heat balance – one decreases while the other increases.

In the discussion of the inter-tube heat fluxes at long timescales it was noted that the magnitude of the flux corresponded to the differences between the fluid temperature in the two legs of the U-tube so that larger fluxes were found in the cases with lower fluid velocities. As the fluid temperature differences are relatively large at the start of the step change in inlet temperature (Figs. 15-17) the inter-tube flux may be thought to be correspondingly large. However, this is not the case. The dynamic change in inter-tube flux has been shown for three fluid velocities in Fig.19. It is apparent that, although the temperature differences between the adjacent fluid is relatively large at the beginning, heat has to be absorbed by the grout present between the pipes before the inter-tube heat flux increases. This suggests that, if short timescale effects are to be considered properly, it is important that dynamic temperature gradients and the thermal mass of the grout between the pipes are considered in any model.

4. Conclusions

Using a multi-block mesh to represent each component of the borehole heat exchanger in three-dimensions and applying a Finite Volume numerical method it has been possible to develop a borehole heat exchanger model that can represent both conduction and fluid circulation processes over both short and long timescales. The model's main purpose, in light of the computational demands of three-dimensional numerical calculations, is to derive step response data for other modeling approaches, to act as a reference model and for use in investigations of three-dimensional and fluid flow physical phenomena.

The model's ability to model the conduction between the components of the borehole and the ground has been verified by reference to thermal resistances calculated using an analytical solution. The model has been shown to be able to reproduce the analytical results to three significant figures.

Comparisons with analytical results have also been used to verify the calculations of fluid transport within the pipes. Calculation of the pipe fluid transport and diffusion processes with a high degree of accuracy probably requires the pipe to be fully discretized and the application of CFD methods. However, this would add considerably to the model's computational demands. This model uses a single layer of cells to represent the fluid and amounts to a one-dimensional treatment of fluid transport. This

approach, when residence time distributions are compared, shows that diffusion is over-predicted by approximately 8%. Experimental validation shows that the model is able to capture the effects of fluid transport and diffusion satisfactorily.

Model validation exercises have been carried out with a BHE experimental data set containing measurements made at relatively high frequency. Short timescale effects have been investigated using data collected during cyclic operation of the experimental heat pump. The behavior of the system has been reproduced very well, including the delayed response due to the transient circulation of fluid in the U-tube. Being able to model such effects is important if interaction between the BHE and the heat pump system controls are to be considered. The model's ability to predict seasonal heat transfer has been investigated using hourly data from the experiment over a period of 18 months. The model is able to predict average outlet temperature very accurately. Monthly net heat transfer has been calculated and shows good agreement with the experimental data and compares favorably with other models.

Numerical study of borehole vertical temperature and heat flux profiles has highlighted the importance of modeling variations in heat transfer with depth and the importance of modeling the dynamic interaction between the pipes and the grout at short timescales. A number of phenomena seem to depend on the flow rate or fluid transit time. In particular, at long timescales borehole heat transfer seems well characterized by the mean fluid and borehole wall temperature if the fluid circulating velocity is reasonably high but at lower flow rates this is not the case. Study of the short timescale dynamics has shown that nonlinearities in the temperature and heat fluxes are noticeable over the whole velocity range of practical interest. The importance of representing the thermal mass of the grout and the dynamic variations in temperature gradient as well as the fluid transport within the borehole has been highlighted.

Acknowledgements

The authors would like to thank J.D. Spitler and S. Hern of the Building, Thermal and Environmental Systems Research Group at Oklahoma State University for provision of the experimental data.

References

- Al-Khoury, R., Bonnier, P. G., Brinkgreve, R. B. J., 2005. Efficient finite element formulation for geothermal heating systems Part I: Steady state. *International Journal for Numerical Methods in Engineering* 63, 988-1013.
- Al-Khoury, R., Bonnier, P. G., 2006. Efficient finite element formulation for geothermal heating systems Part II: Transient. *International Journal for Numerical Methods in Engineering* 67, 725-745.
- Bauer, D., Heidemann, W., Diersch, H.J.G., 2011. Transient 3D analysis of borehole heat exchanger modelling. *Geothermics* 40, 250-260.
- Bennet, J., Claesson, J., Hellstrom, G. 1987. Multipole Method to Compute the Conductive Heat Flows To and Between Pipes In a Composite Cylinder. University of Lund, Sweden.
- Bosworth, R. C. L., 1949. Distribution of reaction time for turbulent flow in cylindrical reactors. *Philosophical Magazine Series* 40, 314-324.
- Cui, P., Yang, H., Fang, Z., 2008. Numerical analysis and experimental validation of heat transfer in ground heat exchangers in alterhantive operation modes. *Energy inn Buildings* 40, 1060-1066.
- De Carli, M., Tonon, M., Zarrela, A., Zecchin, R., 2010. A computational capacity resistance model (CaRM) for vertical ground-coupled heat exchangers. *Renewable Energy* 35, 1537-1550.
- Deng, Z., Rees, S.J., Spitler, J.D., 2005. A model for annual simulation of standing column well ground heat exchangers. *International Journal of Heating, Ventilation, Air-conditioning, and Refrigeration Research* 11(4), 637-656.
- Diersch, H.-J. G., Bauer, D., Heidemann, W., Ruhaak, W., Schatzl, P., 2011. Finite element modeling of borehole heat exchanger systems Part 1. Fundamentals. *Computers & Geosciences* 37, 1122-1135.
- Eskilson, P. 1987. Thermal Analysis of Heat Extraction Boreholes. Doctoral Thesis, University of Lund.
- Fan, D., Rees, S.J., 2009. Modeler report for BESTEST cases GC10a-GC80c: Gems3D version 2.07. Leicester: De Montfort University.
- Ferziger, J. H., Peric, M., 2002. *Computational Methods for Fluid Dynamics*, Springer, Berlin.
- Fisher, D. E., Rees, S. J., Padhmanabhan, S. K., Murugappan, A., 2006. Implementation and Validation of Ground-Source Heat Pump System Models in an Integrated Building and System Simulation Environment. *International Journal of HVAC&R Research* 12(3a), 693-710.
- Gentry, J.E., Spitler, J.D., Fisher, D.E., Xu, X., 2006. Simulation of hybrid ground source heat pump systems and experimental validation, 7th International Conference on System Simulation in Buildings, Liege.
- Gu, Y., O'Neal, D., 1998. Development of an equivalent diameter expression for vertical u-tubes used in ground-coupled heat pumps. *ASHRAE Transactions* 104(2), 347-355.
- Hanby, V. I., Wright, J. A., Fletcher, D. W., Jones, D. N. T., 2002. Modeling the dynamic response of conduits. *International Journal of HVAC&R Research* 8(1), 1-12.

- He, M., 2012. Numerical modelling of geothermal borehole heat exchanger systems. Doctoral Thesis, De Montfort University.
- He, M., Rees, S. J. Shao, L., 2010. Simulation of a domestic ground source heat pump system using a three-dimensional numerical borehole heat exchanger model. *Journal of Building Performance Simulation* 4, 141-155.
- Hellström, G., 1991. Ground Heat Storage: Thermal Analysis of Duct Storage Systems: Part I Theory. Doctoral Thesis, University of Lund.
- Hern, S. A., 2004. Design of an experimental facility for hybrid ground source heat pump systems. Masters Thesis, Oklahoma State University.
- Kummert, M., Bernier, M., 2008. Sub-hourly Simulation of Residential Ground Coupled Heat Pump Systems. *Building Services Engineering Research and Technology* 29, 27-44.
- Li, Z., Zheng, M., 2009. Development of a numerical model for the simulation of vertical U-tube ground heat exchangers. *Applied Thermal Engineering* 29, 920-924.
- Marcotte, D., Pasquier, P., Sheriff, F., Bernier, M., 2010. The importance of axial effects for borehole design of geothermal heat-pump systems. *Renewable Energy* 35, 763-770.
- Molina-Giraldo, N., Blum, P., Zhu, K., Bayer, P., Fang, Z., 2011. A moving finite line source model to simulate borehole heat exchangers with groundwater advection. *International Journal of Thermal Sciences* 50, 2506-2513.
- Mottaghy, D., Dijkshoorn, L., 2012. Implementing an effective finite difference formulation for borehole heat exchangers into a heat and mass transport code. *Renwable Energy*. In press. doi:10.1016/j.renene.2012.02.013.
- Naiker, S.S., Rees, S.J., 2011. Monitoring and Performance Analysis of a Large Non-domestic Ground Source Heat Pump Installation. *Proceedings of CIBSE Technical Symposium 2011*, De Montfort University, Leicester, 6th and 7th September 2011.
- Oppelt, T., Riehl, I., Gross, U., 2010. Modelling of the borehole filling of double U-tube heat exchangers. *Geothermics* 39, 270-276.
- Paul, N. D., 1996. The effect of grout thermal conductivity on vertical geothermal heat exchanger design and performance. Masters Thesis, South Dakota State University.
- Rees, S.J., Spitler, J.D., Xiao, X. 2002. Transient analysis of snow-melting system performance. *ASHRAE Transactions* 108(2), 406-423.
- Rees, S.J., 2009. The PGRID3D parametric grid generation tool user guide, version1.2. Leicester: De Montfort University.
- Sankaranarayanan, K.P., 2005. Modeling, Verification and Optimization of hybrid ground source heat pump system in EnergyPlus. Masters Thesis, Oklahoma State University, Stillwater.
- SEL, 1997. A transient systems simulaion program, user's manual, version 14.2, Solar Energy Laboratory, University of Wisconsin-Madison.
- Signorelli, S., Bassetti, S., Pahud, D., Kohl, T., 2007. Numerical evaluation of thermal response tests. *Geothermics* 36, 141-166.
- Singh A. K., Bhadauria B.S., 2009. Finite difference formula for unequal sub-intervals using lagrange's interpolation formula. *International Journal of Mathematics Analysis* 17(3), 815-827.

- Spitler, J. D., Culline, J., Bernier, M., Kummert, M., Cui, P., Liu, X., Lee, E., Fisher, D. E., 2009. Preliminary intermodel comparison of ground heat exchanger simulation models. 11th International Conference on Thermal Energy Storage - Effstock 2009. Stockholm, Sweden.
- Stone, H. L., 1968. Iterative solution of implicit approximations of multidimensional partial differential equations. *SIAM Journal of Numerical Analysis* 5(3), 530–538.
- Wen, C. Y., Fan, L. T., 1975. *Models for Flow Systems and Chemical Reactors*, New York, Marcel Dekker, Inc.
- Wetter, M., Huber, A., 1997. TRNSYS Type 451: Vertical Borehole Heat Exchanger EWS Model, Version 3.1 - Model Description and Implementing into TRNSYS. Transsolar GmbH, Stuttgart, Germany.
- Xu, X., Spitler, J.D., 2006. Modeling of vertical ground loop heat exchangers with variable convective resistance and thermal mass of the fluid. Proceedings of the 10th International Conference on Thermal Energy Storage-Ecostock 2006, Pomona, NJ.
- Yavuzturk, C., Spitler, J. D., 1999. A Short Time Step Response Factor Model for Vertical Ground Loop Heat Exchangers. *ASHRAE Transactions* 105(2), 475-485.
- Yavuzturk, C., Spitler, J. D., Rees, S. J. 1999. A Transient Two-Dimensional Finite Volume Model for the Simulation of Vertical U-Tube Ground Heat Exchangers. *ASHRAE Transactions* 105(2), 465-474.
- Young, T. R., 2004. Development, Verification, and Design Analysis of the Borehole Fluid Thermal Mass Model for Approximating Short Term Borehole Thermal Response. Masters Thesis, Oklahoma State University.
- Zeng, H.Y., Diao, N.R., Fang, Z.H., 2002. A finite line-source model for boreholes in geothermal heat exchangers. *Heat transfer – Asian research* 31(7), 558-567.

Figures

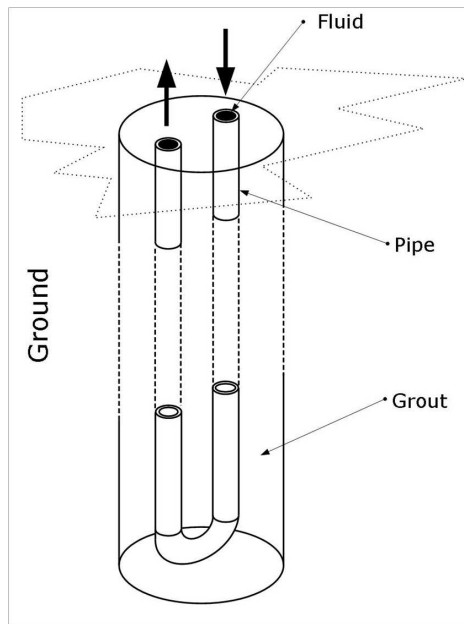


Fig. 1. A single U-tube borehole heat exchanger. Depths are typically 50-150m and bore diameters 100-150mm.

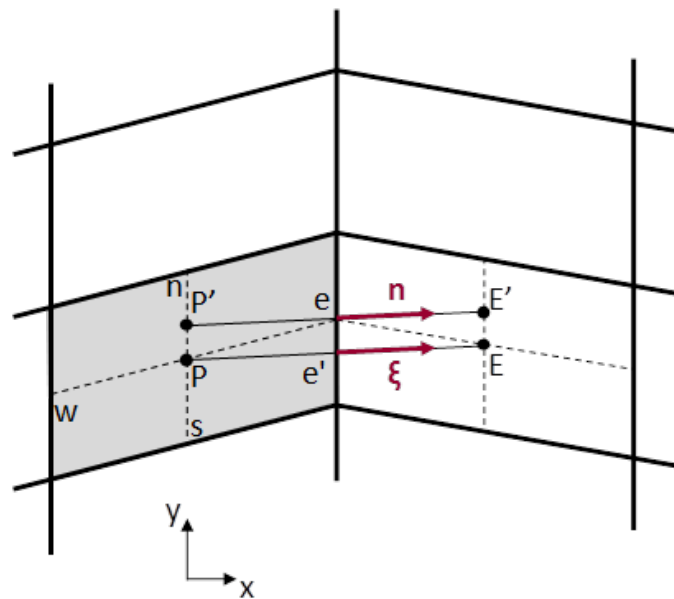


Fig. 2. A diagram of a typical non-orthogonal cell showing the local variables and coordinates defined adjacent a cell face. The east face is highlighted.

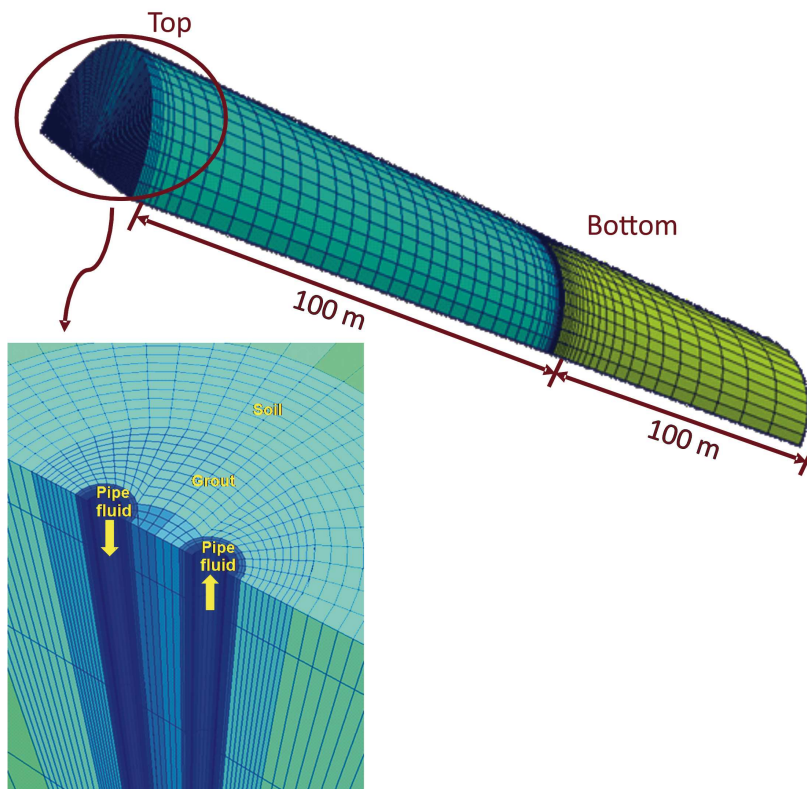


Fig. 3. The numerical mesh used to represent a single borehole heat exchanger.

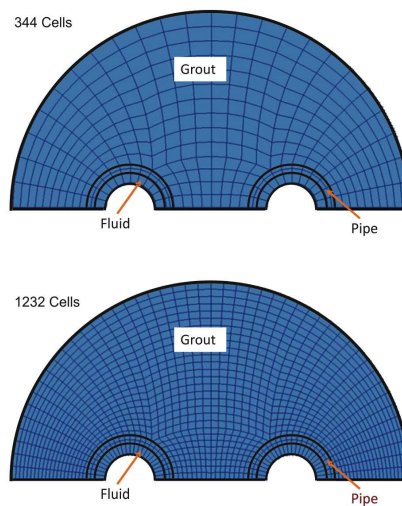


Fig. 4. A horizontal plane through examples of multi-block structured meshes representing a single BHE.

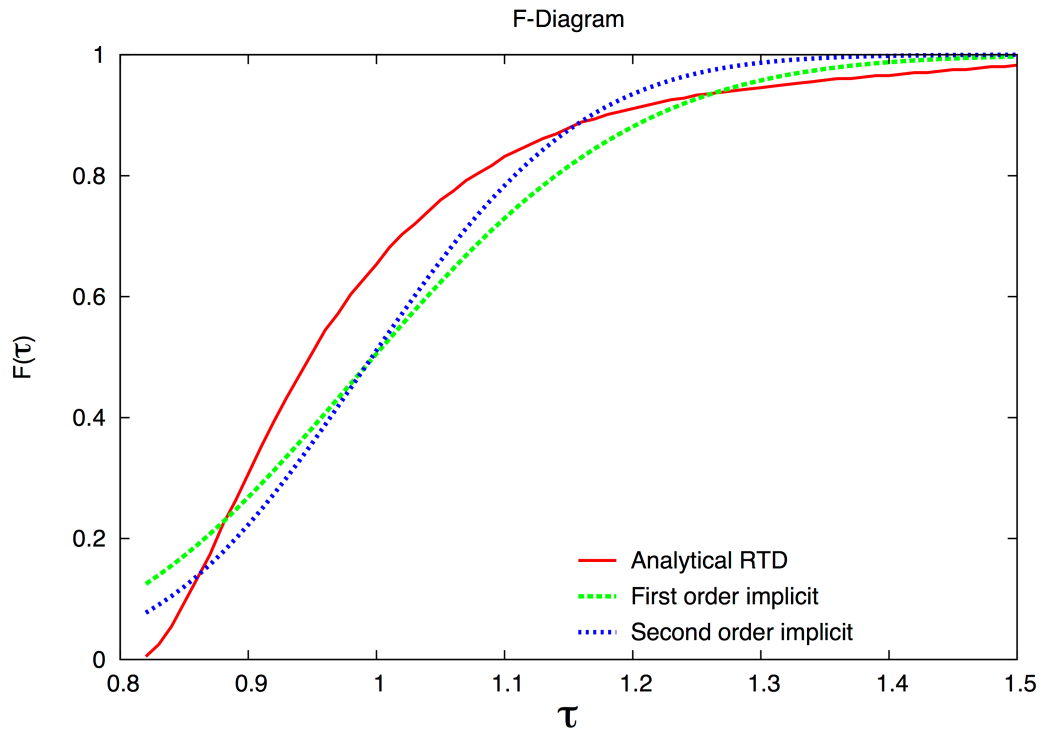


Fig. 5. The predicted residence time distribution compared with the analytical solution. Results for first and second order temporal discretization schemes are shown.

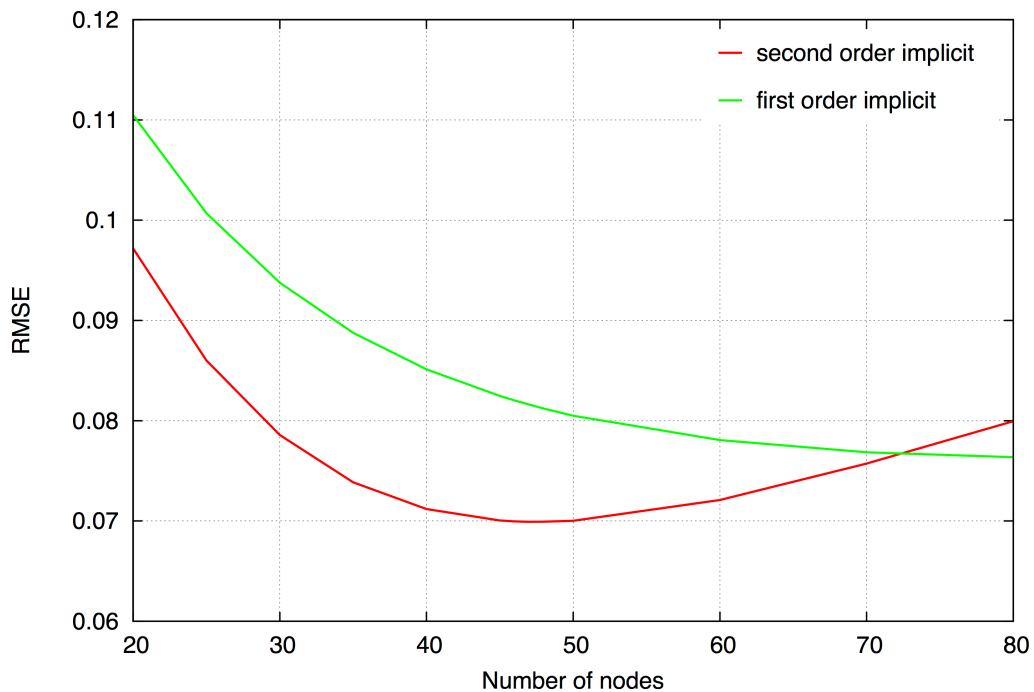


Fig. 6. Differences between the predicted and analytical RTD according to the number of cells used to discretize the pipe.

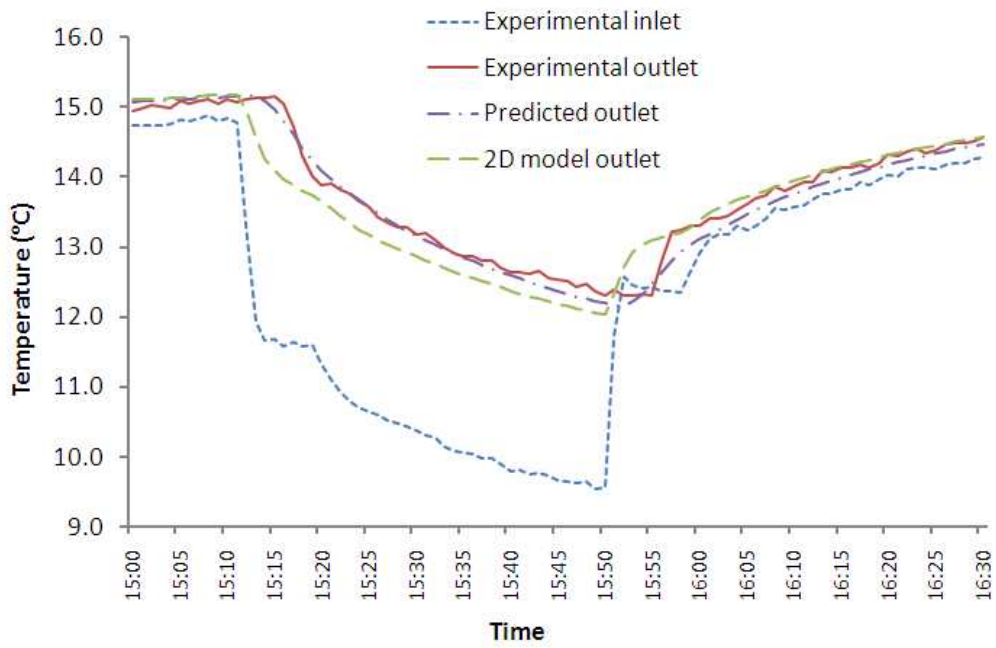


Fig. 7. Experimental and predicted heat exchanger temperatures (15th day of operation, 15:00-16:30).

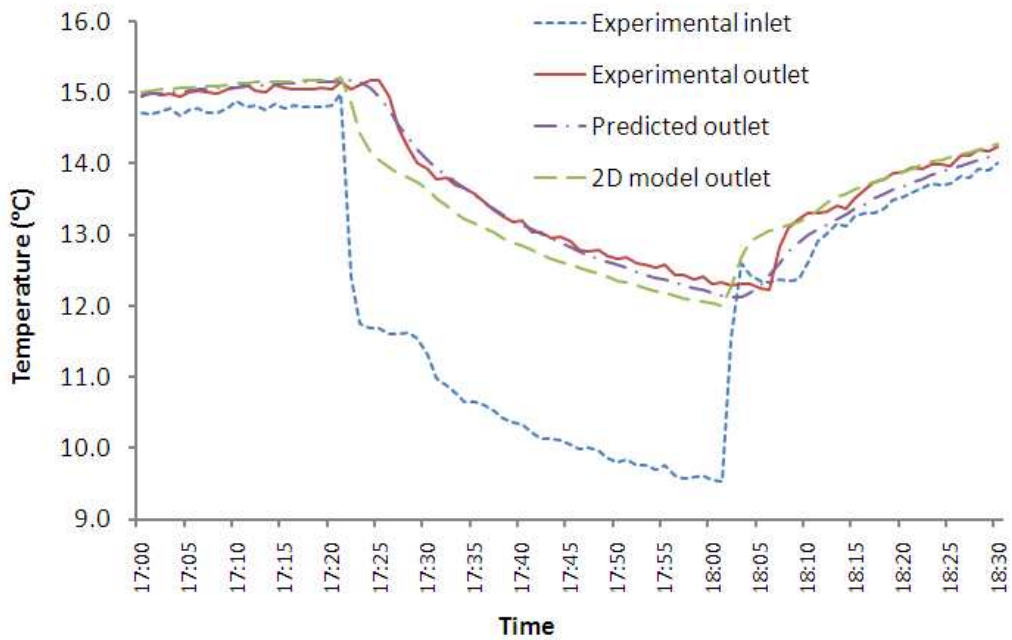


Fig. 8. Experimental and predicted heat exchanger temperatures (15th day of operation, 17:00-18:30).

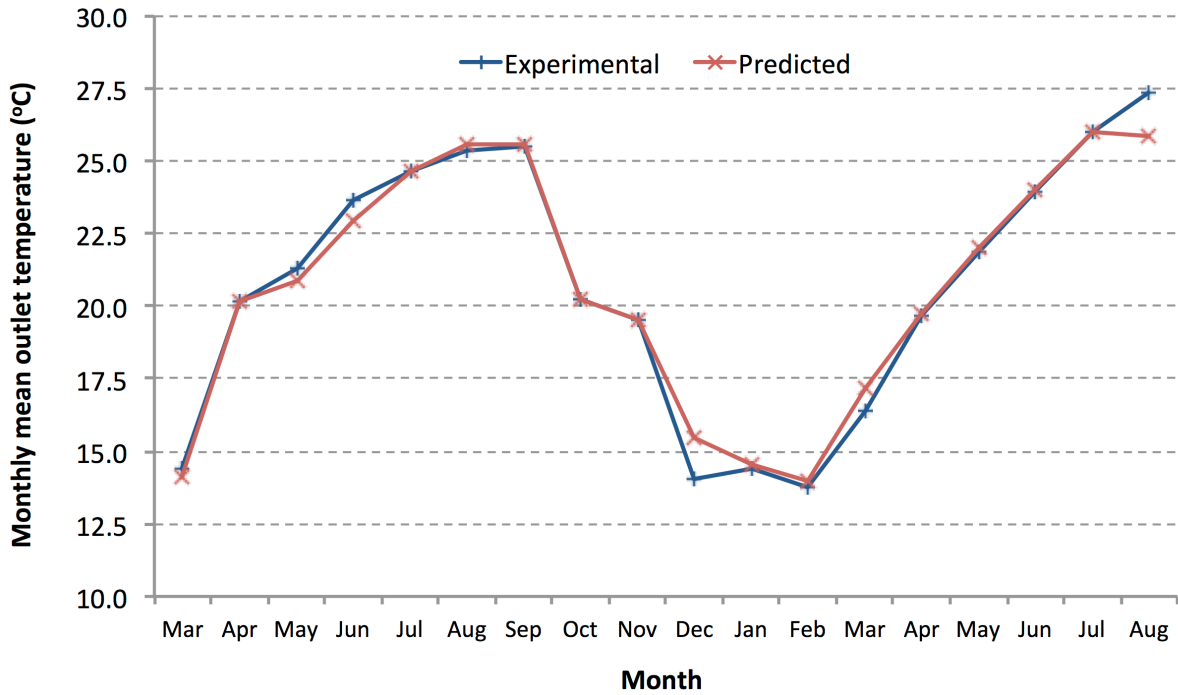


Fig. 9. Measured and predicted monthly mean borehole outlet fluid temperatures.

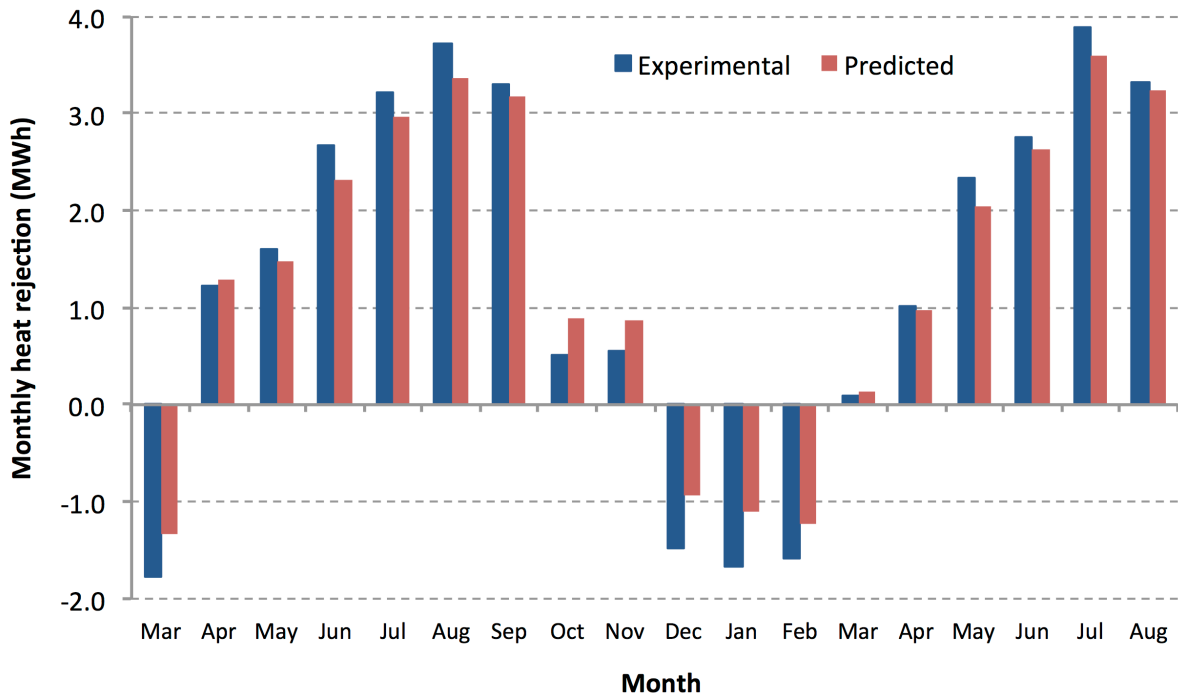


Fig. 10. Measured and predicted monthly net heat exchange (MWh per month). Positive values represent heat rejection.

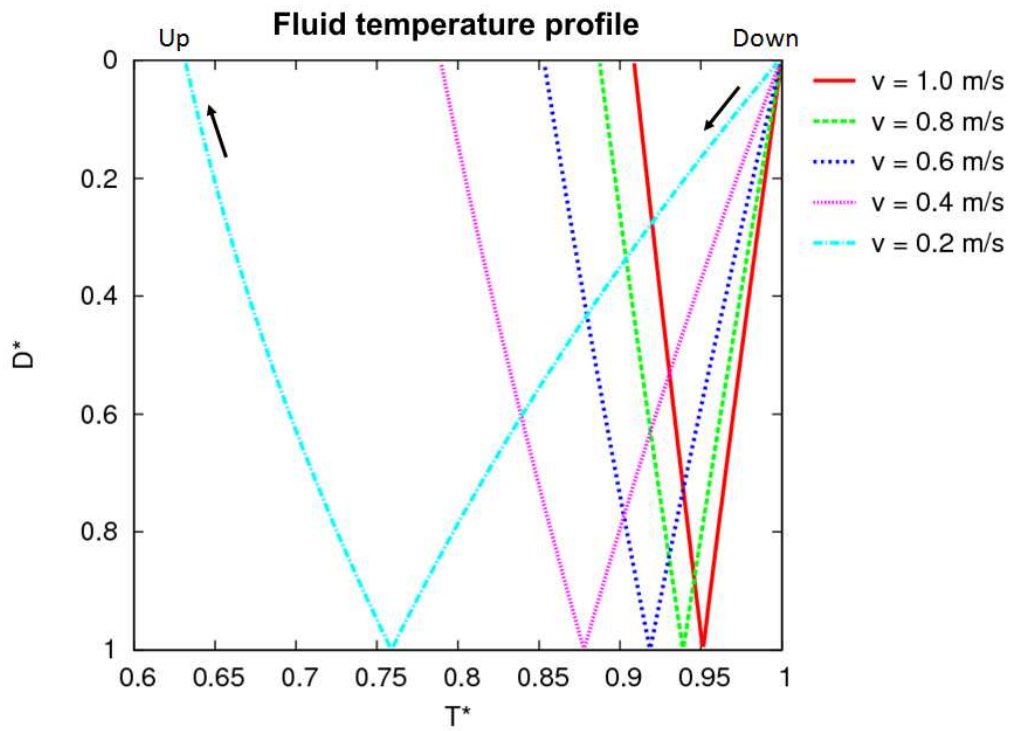


Fig. 11. Steady-state fluid temperature profiles at different fluid velocities.

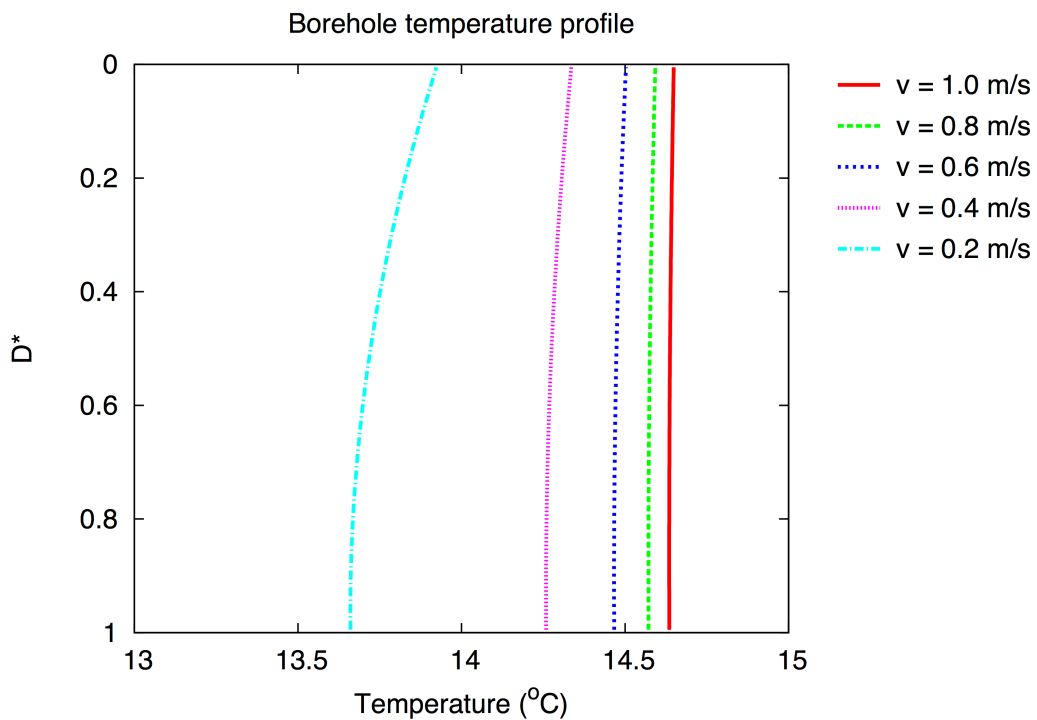


Fig. 12. Steady-state borehole wall temperature profiles at different fluid velocities.

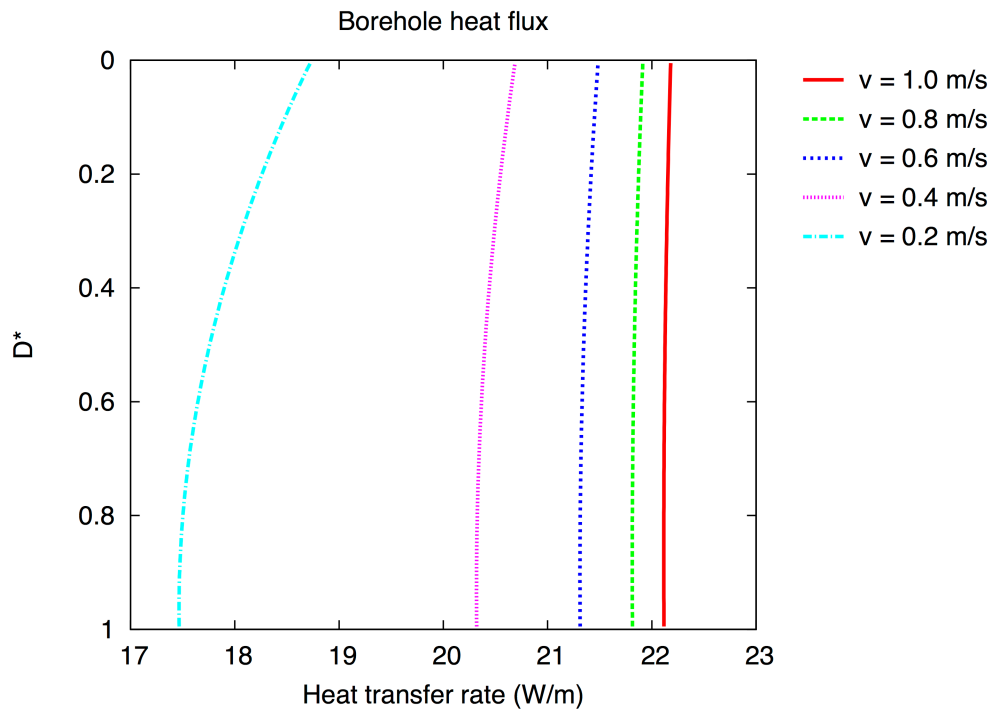


Fig. 13. Steady-state borehole wall heat flux profiles at different fluid velocities.

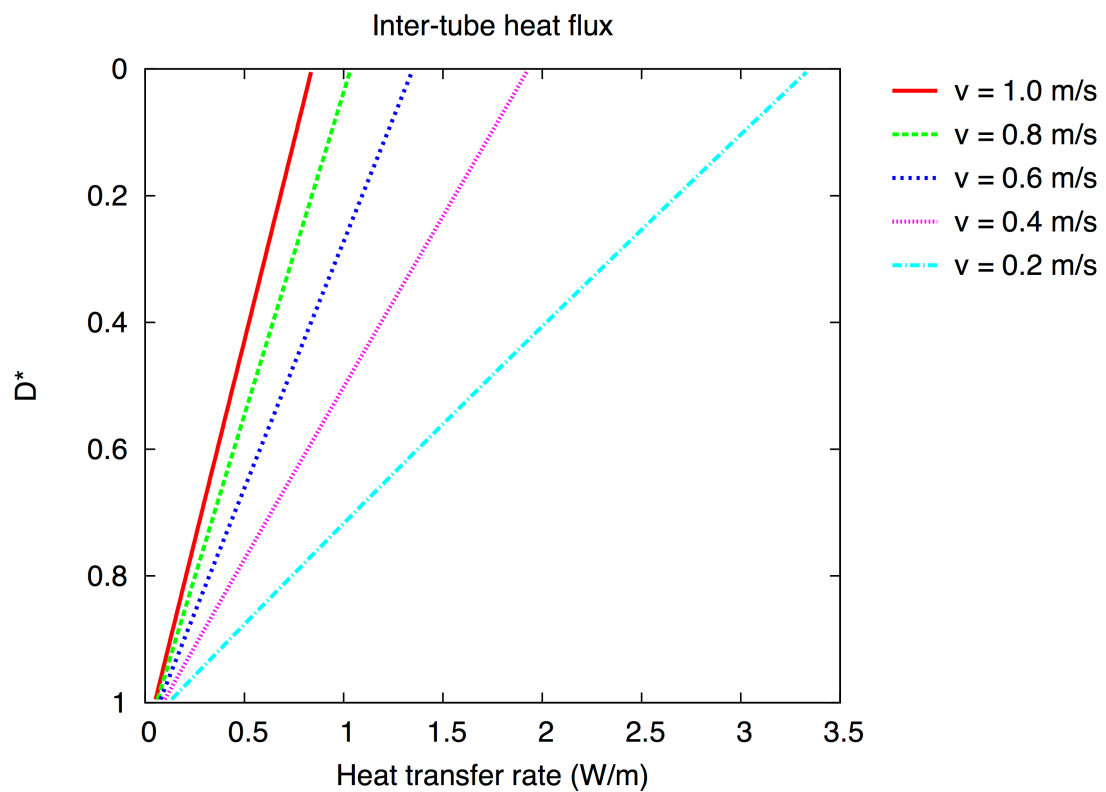


Fig. 14. Inter-tube heat flux along borehole depth at different velocities.

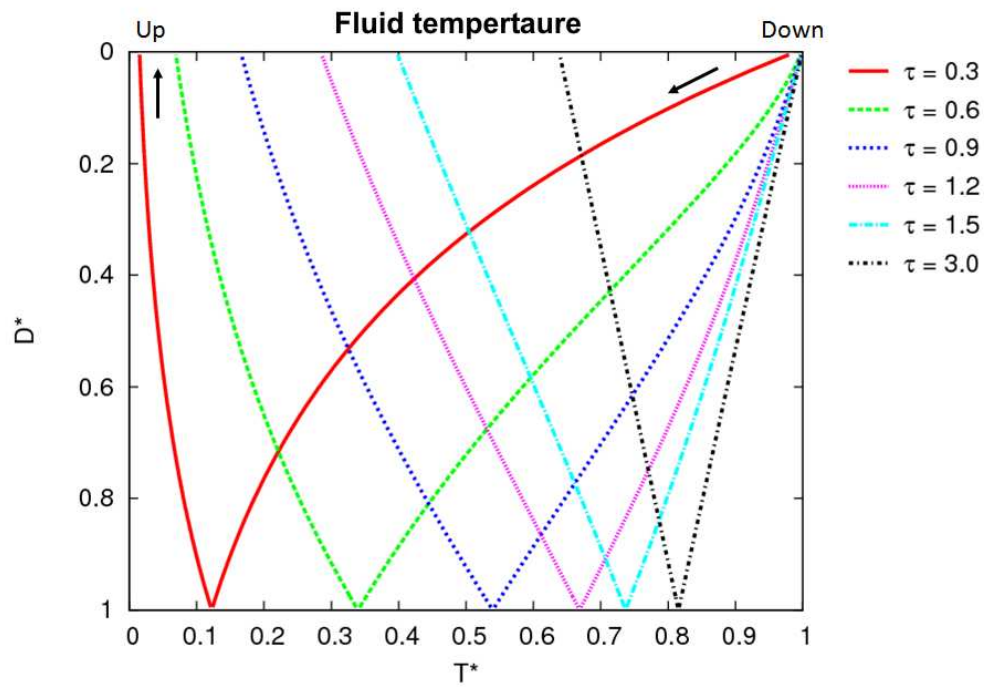


Fig. 15. Fluid temperature profile along the borehole depth ($v=1.0\text{m/s}$, $Re = 25,400$).

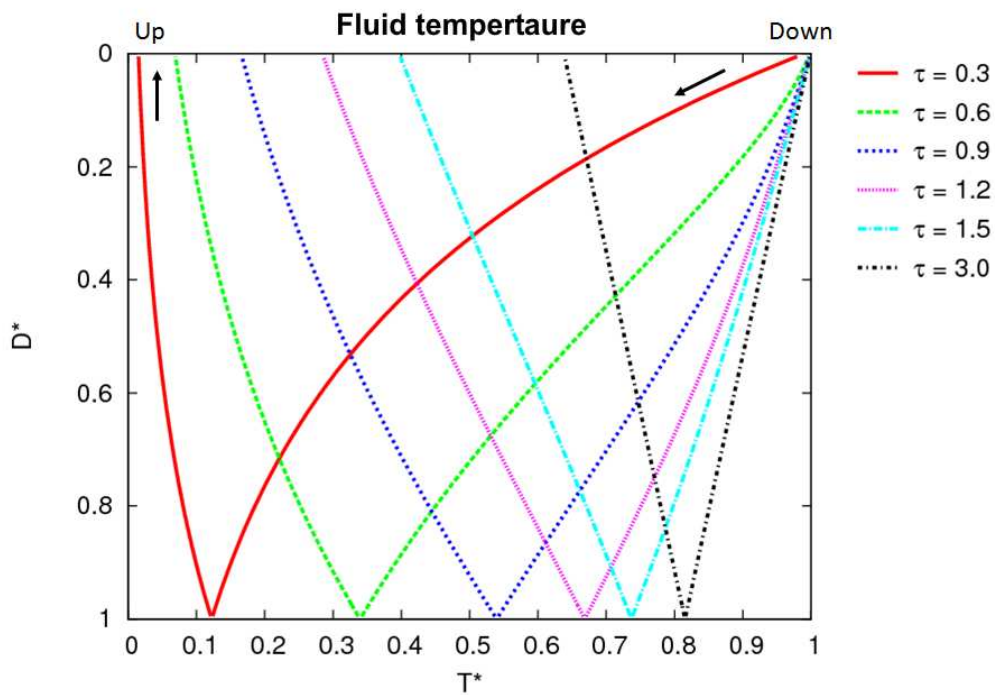


Fig. 16. Fluid temperature profile along the borehole depth ($v=0.6\text{m/s}$, $Re = 15,240$).

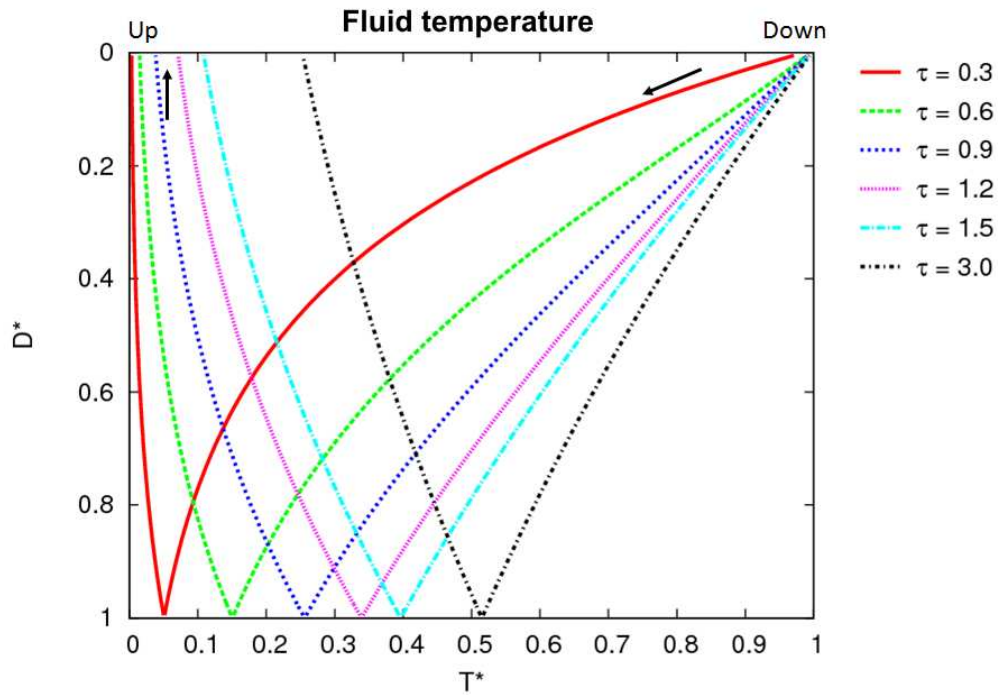


Fig. 17. Fluid temperature profile along the borehole depth ($v=0.2\text{m/s}$, $Re = 5,080$).

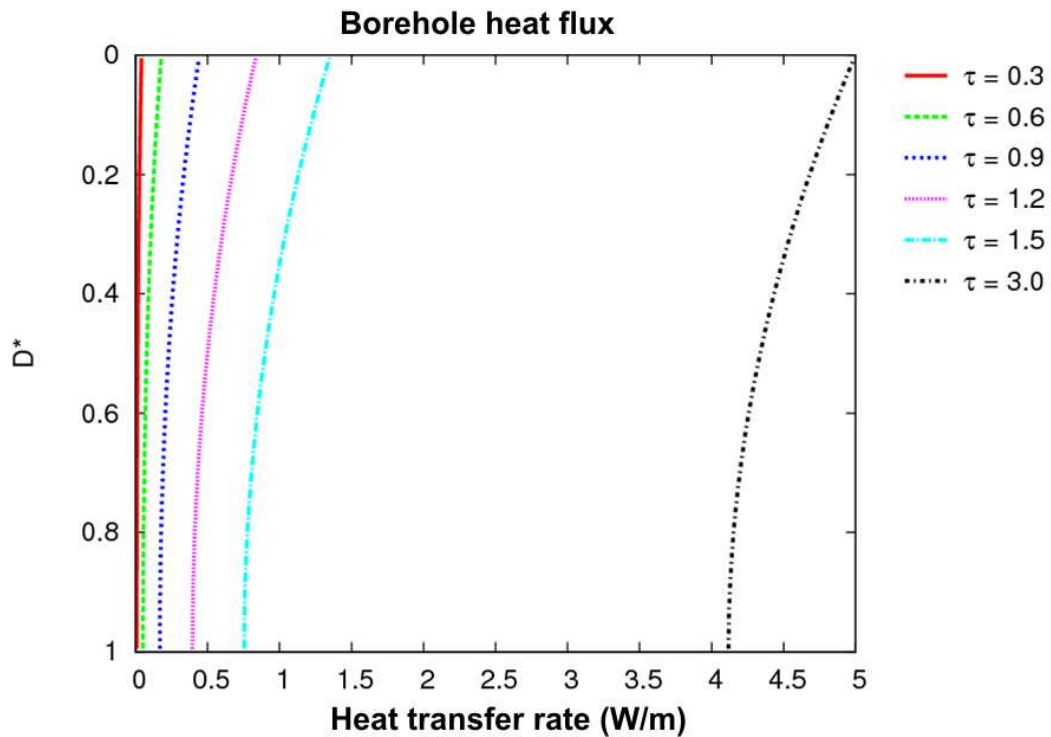


Fig. 18. The borehole wall heat flux profile ($v=0.6\text{m/s}$, $Re = 15,240$).

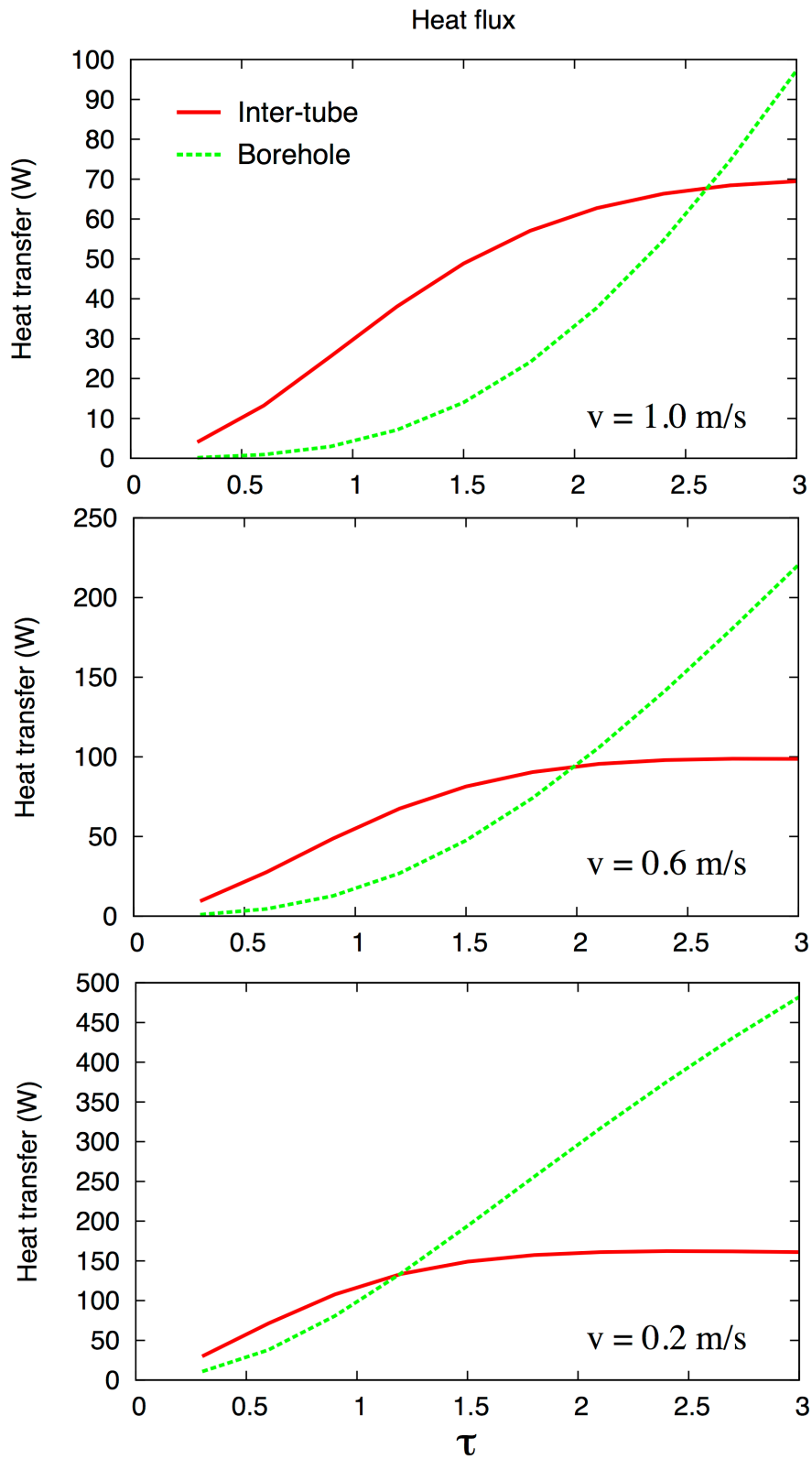


Fig. 19. Comparisons of inter-tube and borehole heat transfer rates after a step change in inlet temperature.

Table 1

BHE dimensions and thermal properties used in calculations of borehole thermal resistances.

Borehole Diameter	D	114.3/152.4	mm
Pipe Inner Diameter	D_{in}	27.4	mm
Pipe Outer Diameter	D_{out}	33.4	mm
Spacing between pipes	L_s	15.8/28.5	mm
Pipe thermal conductivity	Γ_{pipe}	0.39	W/mK
Pipe thermal capacity	ρC_p	1.77	MJ/m ³ K
Grout thermal conductivity	Γ_{grout}	0.75/1.5	W/mK
Grout thermal capacity	ρC_p	3.9	MJ/m ³ K
Ground thermal conductivity	Γ_{ground}	2.5	W/mK
Ground thermal capacity	ρC_p	2.5	MJ/m ³ K
Convection coefficient	h	1690	W/m ² K

Table 2

Calculated borehole thermal resistances.

Borehole Diameter (mm)	Γ_{grout} (W/mK)	No. of Cells	R_b (mK/W)	
			Numerical	Analytical
114.3	0.75	656	0.1827	0.1823
		2,528	0.1825	
		5,688	0.1824	
		10,112	0.1824	
		40,064	0.1824	
		40,448	0.1824	
152.4	0.75	656	0.2221	0.2216
		2,528	0.2218	
		5,688	0.2217	
		10,112	0.2217	
		40,064	0.2216	
		40,448	0.2216	
114.3	1.5	656	0.1160	0.1158
		2,528	0.1161	
		5,688	0.1160	
		10,112	0.1160	
		40,064	0.1160	
		40,448	0.1160	
152.4	1.5	656	0.1347	0.1345
		2,528	0.1347	
		5,688	0.1346	
		10,112	0.1346	
		40,064	0.1346	
		40,448	0.1346	

Table 3

Experimental BHE dimensions and thermal properties.

Borehole Depth	L	74.68	m
Undisturbed ground temp	$T_{initial}$	17.3	°C
Fluid flow rate	\dot{v}	0.212	l/s
Borehole Diameter	D	114.3	mm
Pipe Inner Diameter	D_{in}	21.82	mm
Pipe Outer Diameter	D_{out}	26.67	mm
Borehole Shank Spacing	L_s	20.32	mm
Pipe Thermal Conductivity	Γ_{pipe}	0.3895	W/m.K
Pipe Thermal capacity	ρC_p	1770	KJ/m ³ .K
Grout Thermal Conductivity	Γ_{grout}	0.744	W/m.K
Grout Thermal capacity	ρC_p	3900	kJ/m ³ .K
Ground Thermal Conductivity	Γ_{ground}	2.550	W/m.K
Ground Thermal capacity	ρC_p	2012	KJ/m ³ .K
Fluid Thermal Conductivity	Γ_{water}	0.598	W/m.K
Fluid Thermal capacity	ρC_p	4184	kJ/kg.K
Convection Coefficient	h	2260	W/m ² .K

Table 4.

Circulating fluid design parameters over a range of mean circulating velocities.

Velocity (m/s)	1.0	0.8	0.6	0.4	0.2
Flow Rate (l/s)	0.590	0.472	0.354	0.236	0.118
Reynolds Number	25,400	20,320	15,240	10,160	5,080
Convection Coefficient (W/m ² K)	3,400	2,850	2,260	1,640	940
Nominal Transit Time (s)	200	250	333	500	1,000